Broad-Spectrum Enhancement of Polymer Composite Dielectric Constant at Ultralow Volume Fractions of Silica-Supported Copper Nanoparticles

Guggi Kofod,[†,*] Sebastian Risse,[†] Hristiyan Stoyanov,[†] Denis N. McCarthy,[†] Sergey Sokolov,[‡] and Ralph Kraehnert[‡]

[†]Institute of Physics and Astronomy, University of Potsdam, Karl Liebknecht Strasse 24-25, 14476 Potsdam-Golm, Germany and [‡]Institute of Chemistry, Technical University of Berlin, Strasse des 17. Juni 124, 10623 Berlin, Germany.

ABSTRACT A new strategy for the synthesis of high permittivity polymer composites is demonstrated based on well-defined spatial distribution of ultralow amounts of conductive nanoparticles. The spatial distribution was realized by immobilizing Cu nanoparticles within the pore system of silica microspheres, preventing direct contact between individual Cu particles. Both Cu-loaded and unloaded silica microspheres were then used as fillers in polymer composites prepared with thermoplastic SEBS rubber as the matrix. With a metallic Cu content of about 0.26 vol % in the composite, a relative increase of 94% in real permittivity was obtained. No Cu-induced relaxations were observed in the dielectric spectrum within the studied frequency range of 0.1 Hz to 1 MHz. When related to the amount of conductive nanoparticles, the obtained composites achieve the highest broad-spectrum enhancement of permittivity ever reported for a polymer-based composite.

KEYWORDS: nanocomposite · broad-spectrum permittivity enhancement · metal nanoparticles · uniform spatial arrangement

Polymer materials with high dielectric constant are highly desirable for applications such as capacitors,[1] piezo- and pyroelectric sensors,[2] and field-activated actuators.[3,4] Increasing the permittivity of such materials will enhance their functionality in cases where other required properties, such as mechanical stiffness and electrical breakdown strength, remain mostly unaffected. As reported previously, polymer composites based on conducting particles can show large percolation-related enhancements of the permittivity.[5−8] However, an accompanying increase in low-frequency conductivity and the reduction in breakdown strength of such materials are frequently observed detrimental effects.[9]

In the present paper, a new strategy for permittivity enhancement employing conducting particles dispersed inside silica filler particles is evaluated, in which the permittivity enhancements are obtained at very low volume fractions of the conducting filler. The essence of the strategy is a nonrandom spatial immobilization of the conducting particles within the filler material, such that the conducting nanoparticles possess a narrow distribution in separation distance. This is achieved by synthesizing the conducting metallic Cu nanoparticles ($\phi = 5 \pm 1$ nm) in nonconductive mesoporous silica microspheres ($\phi = 700 \pm 100$ nm) employed as the scaffold. Silica microspheres with and without Cu nanoparticles were mixed into a soft thermoplastic elastomer matrix (SEBS rubber) to produce polymer composites, on which dielectric relaxation spectra were recorded. The presence of Cu nanoparticles was found to result in permittivity enhancement in the entire observable frequency spectrum, without the introduction of loss mechanisms associated with the Cu nanoparticles. This is found by comparing with the Bruggeman dielectric mixing model,[10] which fits well with expectations for the matrix with silica filler but fails to predict the dielectric constant when the Cu nanoparticles are added.

The synthesis route for the Cu-loaded silica microspheres is described shortly in the following (see Supporting Information (SI) for a detailed description of all individual steps and analysis). The silica microspheres, which function as a scaffold for the Cu nanoparticles, were synthesized by co-condensation

* Address correspondence to gkofod@uni-potsdam.de.

Received for review May 29, 2010 and accepted January 19, 2011.

Published online February 08, 2011
10.1021/nn103097q

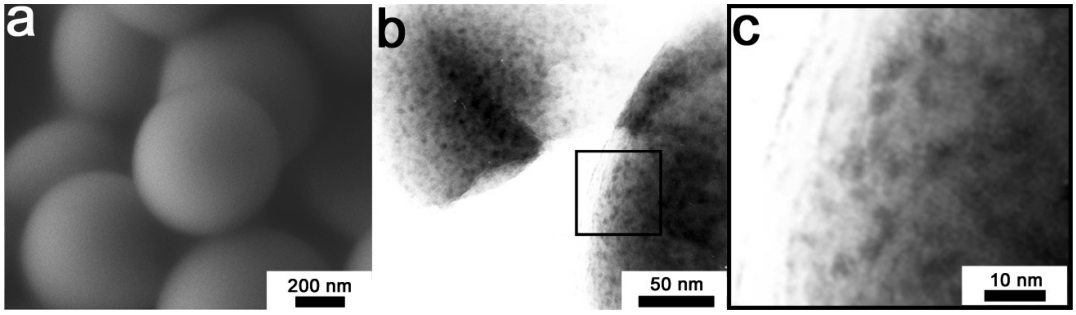

Figure 1. Images of Cu-loaded silica microspheres (P1, low Cu loading) after oxidation−reduction cycle recorded by (a) SEM and (b,c) TEM. The SEM image (a) confirms that no nanoparticles are found on the outer surface of the silica microspheres (see also Supporting Information). The TEM image (b) and further magnified TEM image (c) show the Cu-containing nanoparticles (Cu, CuO, $CuSO_4$) distributed in the mesoporous silica matrix.

of two silane precursors (tetramethylorthosilane "TMOS", mercaptopropyltrimethoxysilane "MPTMS") in a basic water−methanol mixture, with a common surfactant (hexadecyltrimethylammoniumchloride "CTMACl") employed as a structure directing agent.[11] Acid extraction of the template from the as-prepared material yields spherical silica particles (microspheres) with narrow size distribution (700 ± 100 nm) being completely mesoporous (pore diameter *ca.* 2.4 nm). Due to the co-condensation of MPTMS with TMOS, both inner and outer surfaces of the silica microspheres contained thiol groups stemming from MPTMS. The thiol groups facilitate the subsequent adsorption of Cu ions from aqueous solutions of either copper acetate ($Cu(CH_3COO)_2$) or copper nitrate ($Cu(NO_3)_2$).[12,13] Subsequent thermal treatment of the Cu-ion infused microspheres, first in air at 450 °C (calcination), then in diluted hydrogen gas flow (H_2/Ar, 5:95) at 230 °C (reduction) induces the conversion of the adsorbed Cu ions into metallic Cu and its coalescence into Cu nanoparticles (as confirmed *via* a separate study using XRD and XPS analysis; see SI).

Figure 1 shows transmission and scanning electron microscope (SEM and TEM) images of silica microspheres loaded with Cu nanoparticles after calcination and reduction. The silica microspheres after Cu loading are shown in Figure 1a, in which the spheres can be clearly seen, while the Cu nanoparticles are not visible. The presence of Cu nanoparticles with a size of about 5 ± 1 nm in the microspheres is evident from the TEM images in Figure 1b,c. The images show that no Cu nanoparticles are located on the outer surface of the microspheres. Within the microspheres, the Cu nanoparticles are all spatially separated. Moreover, these images suggest that the spatial arrangement of immobilized Cu nanoparticles is nonrandom, which is due probably to the homogeneous dispersion of Cu ions after adsorption as well as a limited range of Cu-ion diffusion during the subsequent thermal treatment, so that Cu nanoparticles form only locally *via* surface diffusion and sintering. A homogeneous distribution of adsorbed Cu ions is explained by binding to the uniformly present SH groups on the surface of MPTMS-derived silica microspheres after template removal *via* acid extraction. The SEM image (a) confirms the narrow size distribution (*ca.* 700 nm diameter) of the silica microspheres as well as the absence of large Cu particles on the outer silica surface.

A number of subsequent analyses were made, including BET, ICP-OES, XPS, and XRD as described in the SI. The density of the pure silica microspheres was estimated from BET data, whereas the total amount of copper in the Cu-loaded silica microspheres was determined with ICP-OES.

As suggested by XPS analysis, a fraction of the Cu is present in the form of CuO and $CuSO_4$. However, relative permittivities of both CuO and $CuSO_4$ are much lower than metallic Cu (which can be taken as infinite in comparison). The relative permittivity of CuO at room temperature was reported as 3−4, increasing to values of not more than 10 in the region below 100 °C.[14] For $CuSO_4$, a value between 7.4 and 10 was reported, where the higher value corresponds to the presence of water.[15] Since the amounts of CuO (0.075 at %) and $CuSO_4$ (0.071 at %) are both lower than that of metallic Cu (0.195 at %), and also their relative permittivities are low, no significant impact on composite permittivity is expected. Using these data and the data presented in SI, the volume fraction of metallic Cu particles in the silica microspheres is calculated as 0.46 vol %.

Composites of thermoplastic SEBS rubber (polystyrene ethylene butadiene styrene with polyolefinic oil, ε_r = 2.3; see SI) with unloaded and Cu-loaded silica microspheres as fillers were prepared for electrical breakdown measurements (described in SI) and dielectric relaxation spectroscopy, with the compositions given in Table 1. For sample preparation, the elastomer was dissolved in toluene and mixed with the respective filler to achieve a filler fraction of 55, such that for sample C the content of metallic Cu in the composite volume amounted to 0.26 vol % (see also SI).

Dielectric relaxation spectroscopy (DRS) was performed on samples A (SEBS), B (SEBS with unloaded SiO_2), and C (SEBS with Cu-loaded SiO_2) at different temperatures (see Figure 2), with temperatures from 233 to 393 K in steps of 10 K, in the frequency range

from 0.1 Hz to 1 MHz, with repeatable results. Shown are the values of the real (top row) and imaginary (bottom row) components of the complex relative permittivity, $\varepsilon\sim = \varepsilon' - i\varepsilon''$.

It was found that composite samples were highly sensitive to the influence of air humidity. An experiment was made in which a sample of composition B (SEBS-SiO_2) was exposed to ambient conditions with a temperature of 22 °C and an average air humidity of 70% for 10 days prior to DRS, whereas another sample was dried in an exsiccator at 50 °C for 5 days. Comparing DRS of dried and nondried SEBS-SiO_2 (see SI) reveals an enormous difference in the permittivity spectra, that is, a large relaxation peak appearing in the spectra for the nondried sample. To exclude humidity-related effects, all samples were dried several days in an exsiccator at 50 °C prior to DRS analysis, giving rise to the spectra shown in Figure 2.

RESULTS

In Figure 2, all three real spectra (a, c, e) are characterized by a large flat plateau. Only in the region of particularly low frequencies and high temperatures is a deviation found, which can be reconciled with the universal behavior common for electrically insulating polymers.[16] The imaginary response shows no relaxation peaks and was found to increase with decreasing frequency and increasing temperature for all samples (Figure 2b,d,f), which is also typical for insulating polymers.[17] Interestingly, a large global increase in the plateau value of the real permittivity is found, both when going from sample A to B and when going from B to C, the physical background of which will be discussed in detail further below.

Electrical breakdown experiments (see SI) were carried out on samples A, B, and C. The results indicate that the breakdown field of pure SEBS drops when adding the unloaded silica microspheres, from approximately 90.1 ± 14.8 to 27.0 ± 7.9 V/μm, which is almost identical to the value for pure silica. The breakdown field when using copper-loaded silica microspheres is approximately 22.8 ± 6.9 V/μm, within experimental error the same value as for unloaded microspheres. It is therefore concluded that the presence of copper nanoparticles does not influence the breakdown properties of the composite. Since percolation leads to strong reductions in electrical breakdown strength already at very low loading,[9] it can be inferred that percolation effects are not present in this composite. In other words, the electrical breakdown measurements strongly indicate that copper nanoparticles are well-separated from each other, with almost uniform separation between nearest neighbor particles.

An investigation of the ac conductivity, $\sigma'(\omega) = \omega\varepsilon_0\varepsilon''(\omega)$, shows whether samples are inherently conducting or insulating. A model by Dyre and Schrøder[18] for ac conductivity due to transport in a disordered

TABLE 1. Composition of Samples for Dielectric Spectroscopy

sample	description	mesoporous SiO_2, vol %	metallic Cu, vol %
A (SEBS)	pure SEBS	0	0
B (SEBS-SiO_2)	SEBS and silica microspheres	55	0
C (SEBS-SiO_2-Cu)	SEBS and Cu-loaded silica microspheres	55	0.26

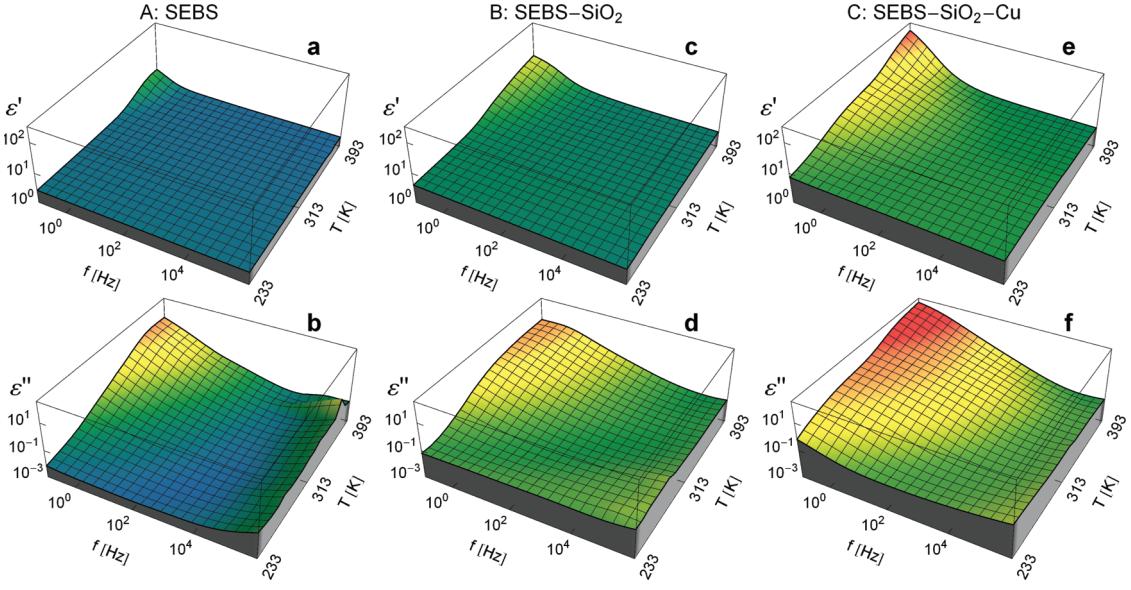

Figure 2. Dielectric relaxation spectra with temperature variation of samples A (SEBS), B (SEBS-SiO_2), and C (SEBS-SiO_2-Cu) (from left to right), showing increases in both real (top row) and imaginary parts (bottom row) of the permittivity from A to B to C. The increases are seen to be *global*, raising the real permittivity by the same amount throughout the entire frequency and temperature range, with no relaxation peaks in the imaginary part.

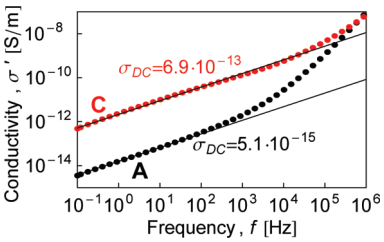

Figure 3. Conductivity of samples A (SEBS) (black) and C (SEBS-SiO_2-Cu) (red), which are found to have the same slope $n = 0.63$ in the log−log representation, corresponding in both cases to transport in a disordered solid and not to bulk metallic transport.

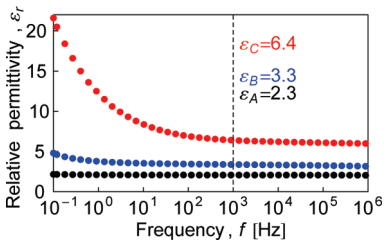

Figure 4. Permittivity spectra of samples A (black), B (blue), and C (red). The increase in the plateau permittivity from A to B can be reconciled with the Bruggeman equation, while from B to C, the increase is far larger than predicted.

solid finds a universal frequency dispersion behavior, written as

$$\sigma'(\omega) = \sigma_{DC}\left(\frac{\omega}{\omega_c}\right)^n, \text{ for } \omega \gg \omega_c \qquad (1)$$

The model is valid when the measurement frequency is near the critical frequency, ω_c, where conductivity processes switch from purely charge carrier mediated to capacitive switching.[18] For a regular conductor, $n = 0$, a perfect insulator has $n = 1$, while a disordered solid has $0.6 < n < 1.0$.

The model (eq 1) was fitted to the conductivity spectra of samples A (SEBS) and C (SEBS-SiO_2-Cu) (Figure 3), in both cases returning $n = 0.63$ corresponding with a disordered solid[18] (the experimental curve deviates from the theoretical expression above 1 kHz for sample A due to limitations in the measurement equipment, effects of which can also be seen in the imaginary permittivity of A in the upper frequency range, Figure 2). The fit also returns the upper estimates for σ_{DC}, corresponding in both cases to well-insulating polymers. Since n is equal for A and C, the mechanism of conductivity is similar, in both cases governed by disordered transport. For A, the disorder is given by the domain structure in the physically cross-linked thermoplastic elastomer,[19] while the upward shift in dc conductivity is explained by the presence of the silica material which leads to further disordered transport mechanisms. Finally, since $n = 0.63$ is far above 0, it can be concluded that the metallic Cu nanoparticles do not contribute significantly to conductivity and are therefore not in direct electrical contact throughout the bulk composite.

The changes in real permittivity from A to B to C are highlighted in Figure 4, showing room temperature spectra for all three samples. As mentioned above, a strong dispersion is found at frequencies below 100 Hz, a universal behavior typical for polymers.[17,19] Hence, we can conclude that the dispersions are due to processes arising within the polymer, whereas the global upward shift in real permittivity is due to an increase in the background permittivity, caused by high-frequency responses of the filler particles. At 1 kHz, the value of real permittivity increases from pure polymer ($\varepsilon_A = 2.3$) over polymer with 55 vol % pure silica ($\varepsilon_B = 3.3$) to polymer with 55 vol % silica with Cu nanoparticles ($\varepsilon_C = 6.4$).

A number of mixing models[4,20] can predict the permittivity of composites, based on the amounts of matrix and filler as well as their respective permittivities. The commonly used Bruggeman model[10] makes good predictions[4]

$$1 - v = \frac{\varepsilon_2 - \varepsilon_c}{\varepsilon_2 - \varepsilon_1}\left(\frac{\varepsilon_1}{\varepsilon_c}\right)^{1/3} \qquad (2)$$

where v is the volume fraction of the filler and ε_2, ε_1, and ε_c are the permittivities of the filler, the matrix, and the composite, respectively. Infinite filler permittivity can be assumed for electrically conductive particles.

The relative increase in permittivity due to addition of pure silica can be reconciled with the Bruggeman prediction (eq 2), from which a value for the filler permittivity of 4.3 is calculated. This value compares well with that of pure glass, which has a real permittivity of 3.8−9.0 (depending upon composition[15]); in this case, 1 SH bond is present for every 6 Si atoms. Since the dipole moment of this bond is relatively low, this could possibly explain the slight elevation of the filler permittivity.

The value of the real permittivity for the SEBS-SiO_2-Cu composite of 6.4 cannot be reconciled with the Bruggeman model, as will be shown now. The content of metallic Cu in the filler particles amounts to 0.46 vol %, corresponding to 0.26 vol % in the composite. Using the Bruggeman equation, assuming infinite permittivity for the metallic particles, the predicted composite permittivity would be 3.34, which is far below the observed 6.4. Also, the Bruggeman equation implies a permittivity of 13.5 of the Cu-loaded silica microspheres, which again according to the Bruggeman equation would require 32 vol % of metallic Cu, which is clearly not the case. In conclusion, the presence of metallic Cu nanoparticles in ultralow amounts leads to a very high increase in permittivity, far above what is expected from classical mixing models.

As has been just demonstrated, the impact of the metal nanoparticles on broadband real permittivity is high compared to the volume fraction present. A figure

TABLE 2. FOM Calculated for Different Polymer/Conductive Filler Composites

matrix/filler	*v* filler	FOM @1 kHz	FOM @1 MHz
PVDF/Ni[6,a]	0.05	10.3	47.6
VMQ/CB[21,b]	0.005	50.1	58.0
PBT/SWCNT[22,c]	0.01	0.8	8.7
SEBS/CB[9,d]	0.005	44.3	40
PE/Fe[23,e]	0.1	4.6	4.5
SEBS-SiO_2-Cu	0.0026	344.8	344.5

[a] Poly(vinylidene difluoride)/Ni. [b] Vinyl silicone rubber/carbon black. [c] Poly(butylene terephthalate)/single-wall carbon nanotubes. [d] Poly(styrene-*co*-ethylene-*co*-butylene-*co*-styrene)/carbon black. [e] Polyethylene/Fe.

of merit (FOM) can be defined, which describes the relative enhancement of permittivity with respect to the volume fraction of conducting particles *v*

$$\mathrm{FOM} = \frac{\left(\frac{\varepsilon_c - \varepsilon_1}{\varepsilon_1}\right)}{v} \quad (3)$$

FOMs are listed in Table 2. For comparison, data have been extracted from literature.[6,9,21−23] For a proper comparison, the permittivity values at the lowest filler concentrations were chosen, and FOMs were calculated for both 1 kHz and 1 MHz to accommodate for low-frequency dispersion (Table 2). In all cases quoted, higher FOMs are found at higher filler ratios; however, here the focus is on comparing systems in which the lowest amount of filler provides the highest possible permittivity enhancement. Hence, the values quoted pertain to composite systems which are far from the percolation threshold, as is the case for the system discussed here. As can be observed directly, the FOM for this system is almost 1 order of magnitude higher than the second highest listed.

We now discuss possible mechanisms behind the observed permittivity increase. A first explanation is suggested based on a volumetric effect, in which each of the metal clusters contributes to the permittivity through its higher dipole moment (as compared to the matrix). The classical polarizability of a metal sphere[24,25] is $\alpha = 3V$, where V is the volume of the particle, hence, permittivity scales with the volume of the particle. In our case, if the same amount of Cu is present as one large particle, or as many small nanoparticles, this will not change the permittivity of the whole. Further, since the total amount of metallic Cu material in the composite comprises only 0.26 vol %, the overall effect on the composite permittivity due to the classical dipole moment of the metal nanoparticles can be neglected.

As mentioned above, the apparent permittivity of the Cu-loaded silica microspheres was $\varepsilon_r = 13.5$, a value much higher than predicted by the Bruggeman theory; hence other mechanisms must be invoked. Classical percolation theory for randomly oriented, spherical conducting particles suggests a 3D percolation threshold of ≈15 vol %.[26] As seen from the TEM analysis (Figure 1), the Cu nanoparticles are close to spherical, yet their amount is just 0.46 vol %, and they are not randomly distributed; hence classical percolation cannot explain the increase in permittivity. Also, the electrical breakdown experiments did not show a significant drop in electrical breakdown field (see SI), which is otherwise taken as a strong indication of percolation.[9] In summary, both TEM and electrical breakdown measurements strongly indicate the absence of percolation.

The average distance between the equally spaced metallic particles can be estimated based on their size and concentration, suggesting an average particle−particle separation of ≈55 nm. This separation is somewhat too high to permit the occurrence of tunneling effects; however, if there are local fluctuations in size and interparticle separation, percolation-type enhancement might still be a possible explanation. Another tunneling-based explanation could be the Gor'kov−Eliashberg (GE) effect,[27] relying on conducting nanosized domains in a chain-like arrangement, separated by insulating barriers, which could lead to very high permittivity along the chain. However, as mentioned by Halperin,[25] the existence of the effect remains dubious. As a final suggestion, the effects of surface plasmon resonances (SPR) might be invoked as being responsible for the permittivity enhancement.[25] SPR was, for instance, observed using UV−vis spectroscopy in gold nanoparticles with a size distribution of 3.5 ± 0.6, embedded in a polystyrene matrix.[28] Hence, SPR would lead to relaxation at frequencies much higher than those observable using DRS, with a corresponding increase in real permittivity. We observed such an effect experimentally applying DRS to the composite (C) SEBS-SiO_2-Cu.

An interesting feature of the permittivity enhancement is the fact that it appears globally in the entire frequency range, leading to an upward shift in permittivity for all temperatures and frequencies. In a general dielectric relaxation process, the real and imaginary (loss) parts of the permittivity are linked by the Kramers−Kronig relation,[17] which states that the integrated area under the loss curve equals the real permittivity, as schematically illustrated in Figure 5. As indicated in Figure 5, enhancement can lead to large losses in the usage interval; hence it would be of large practical importance to shift such losses to higher frequencies. In the present case, no relaxation is found in the spectra, apart from the unrelated low-frequency dispersion discussed previously; hence the responsible enhancement has a relaxation time much faster than any time scale in the experiment, $\tau \approx 1/f_{max} = 1\ \mu s$, where $f_{max} = 1$ MHz is the highest measurement frequency. The experimental observation made here is consistent with the interpretation of SPR being responsible for the observed enhancement of real

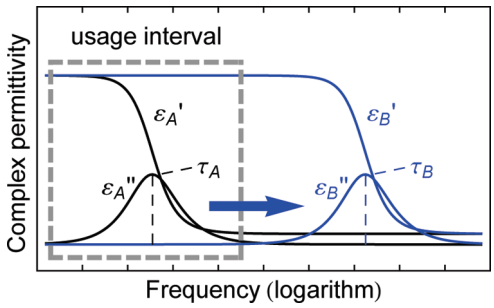

Figure 5. Relaxation process leads to enhancement in real permittivity with corresponding loss. Shifting the relaxation out of the usage interval reduces losses while still enjoying the benefits of the enhancement in real permittivity.

permittivity (the SPR peak lies at ≈600 nm, ~0.5 THz for Cu nanoparticles[29]).

In conclusion, mesoporous silica microspheres were synthesized and loaded with metallic Cu nanoparticles of 5 ± 1 nm, placed with fairly uniform interparticle distances. The Cu content in the silica microspheres amounted to 0.46 and 0.26 vol % in an SEBS-SiO_2-Cu composite. Dielectric analysis of SEBS and SEBS-SiO_2 as well as SEBS-SiO_2-Cu composites revealed an extremely high impact of the Cu nanoparticles on permittivity, that is, an improvement from the 3.3 of the silica-filled composite to a value of 6.4 when immobilized Cu nanoparticles are added. A figure of merit was established, showing that the impact of the nanoparticles was much larger than hitherto observed for similar systems of conducting filler composites. The high impact for such a low amount of material is difficult to reconcile with common theories, such as the polarizability of metal spheres, the Bruggeman mixing rule, or classical percolation theory. Remarkably, the permittivity enhancement was found to be global, applying in the entire measurement range, a result which could be of great importance for a number of applications. We propose that the effect is induced due to the small size of the particles, as well as their uniform spatial distribution in the mesoporous silica microspheres. Hence, we propose that a mechanism based on surface plasmon resonances at frequencies above the DRS measurement range could provide an explanation for the observed enhancement in permittivity.

Acknowledgment. The authors acknowledge NanoFutur grants from the German BMBF, in the WING program (FKZ 03X5511 and FKZ 03X5517A). We thank K. Weh for help in the lab, and M. M. Pohl for TEM analysis. The authors are grateful for valuable discussions with P. Frübing and S. Lanceros-Mendez.

Supporting Information Available: Additional experimental details. This material is available free of charge *via* the Internet at http://pubs.acs.org.

REFERENCES AND NOTES

1. Rao, Y.; Ogitani, S.; Kohl, P.; Wong, C. Novel Polymer–Ceramic Nanocomposite Based on High Dielectric Constant Epoxy Formula for Embedded Capacitor Application. *J. Appl. Polym. Sci.* **2002,** *83*, 1084–1090.
2. Pelaiz-Barranco, A.; Marin-Franch, P. Piezo-, Pyro-, Ferro-, and Dielectric Properties of Ceramic/Polymer Composites Obtained from Two Modifications of Lead Titanate. *J. Appl. Phys.* **2005,** *97*, 034104.
3. Carpi, F.; De Rossi, D. Improvement of Electromechanical Actuating Performances of a Silicone Dielectric Elastomer by Dispersion of Titanium Dioxide Powder. *IEEE Trans. Dielectr. Electr. Insul.* **2005,** *12*, 835–843.
4. Gallone, G.; Carpi, F.; De Rossi, D.; Levita, A.; Marchetti, G. Dielectric Constant Enhancement in a Silicone Elastomer Filled with Lead Magnesium Niobate–Lead Titanate. *Mater. Sci. Eng., C* **2007,** *27*, 110–116.
5. Rao, Y.; Wong, C. Ultra High Dielectric Constant Epoxy Silver Composite for Embedded Capacitor Application. *Proc. IEEEECTC* **2002,** 920–923.
6. Dang, Z.; Lin, Y.; Nan, C. Novel Ferroelectric Polymer Composites with High Dielectric Constants. *Adv. Mater.* **2003,** *15*, 1625–1629.
7. Saha, S. K. Nanodielectrics with Giant Permittivity. *Bull. Mater. Sci.* **2008,** *31*, 473–475.
8. Carpi, F.; Gallone, G.; Galantini, F.; De Rossi, D. Silicone-Poly(hexylthiophene) Blends as Elastomers with Enhanced Electromechanical Transduction Properties. *Adv. Funct. Mater.* **2008,** *18*, 235–241.
9. Stoyanov, H.; Mc Carthy, D. N.; Kollosche, M.; Kofod, G. Dielectric Properties and Electric Breakdown Strength of a Subpercolative Composite of Carbon Black in Thermoplastic Copolymer. *Appl. Phys. Lett.* **2009,** *94*, 232905.
10. Bruggemann, D. G. Berechnung verschiedener physikalischer Konstanten von heterogenen Substanzen. *Ann. Phys.* **1935,** *24*, 636–679.
11. Nakamura, T.; Yamada, Y.; Yano, K. Direct Synthesis of Monodispersed Thiol-Functionalized Nanoporous Silica. *J. Mater. Chem.* **2007,** *17*, 3726–3732.
12. Lee, B.; Kim, Y.; Lee, H.; Yi, J. Synthesis of Functionalized Porous Silicas *via* Templating Method as Heavy Metal Ion Adsorbents: The Introduction of Surface Hydrophilicity onto the Surface of Adsorbents. *Microporous Mesoporous Mater.* **2001,** *50*, 77–90.
13. Bois, L.; Bonhomme, A.; Ribes, A.; Pais, B.; Raffin, G.; Tessier, F. Functionalized Silica for Heavy Metal Ions Adsorption. *Colloids Surf., A* **2003,** *221*, 221–230.
14. Zheng, X. G.; Sakurai, Y.; Okayama, Y.; Yang, T. Q.; Zhang, L. Y.; Yao, X.; Nonaka, K.; Xu, C. N. Dielectric Measurement To Probe Electron Ordering and Electron-Spin Interaction. *J. Appl. Phys.* **2002,** *92*, 2703–2708.
15. *Handbook of Chemistry and Physics*, 72nd ed.; Lide, D. R., Ed.; CRC Press: Boca Raton, FL, 1991.
16. Jonscher, A. K. The "Universal" Dielectric Response. *Nature* **1977,** *267*, 673–679.
17. Jonscher, A. K. *Dielectric Relaxations in Solids*; Chelsea Dielectric Press: London, 1983.
18. Dyre, J.; Schroder, T. Universality of AC Conduction in Disordered Solids. *Rev. Mod. Phys.* **2000,** *72*, 873–892.
19. *Block Copolymers*; Calleja, F. J. B., Roslaniec, Z., Eds.; Marcel Dekker: New York, 2000.
20. Jylhä, L.; Sihvola, A. Equation for the Effective Permittivity of Particle-Filled Composites for Material Design Applications. *J. Phys. D: Appl. Phys.* **2007,** *40*, 4966–4973.
21. Dang, Z.-M.; Xia, B.; Yao, S.-H.; Jiang, M.- J.; Song, H.-T.; Zhang, L.-Q.; Xie, D. High Dielectric-Permittivity High-Elasticity Three-Component Nanocomposites with Low Percolation Threshold and Low Dielectric Loss. *Appl. Phys. Lett.* **2009,** *94*, 042902.
22. Nogales, A.; Broza, G.; Roslaniec, Z.; Schulte, K.; Sics, I.; Hsiao, B.; Sanz, A.; Garcia-Gutierrez, M.; Rueda, D.; Domingo, C..;*et al.*Low Percolation Threshold in Nanocomposites Based on Oxidized Single Wall Carbon Nanotubes and Poly(butylene terephthalate). *Macromolecules* **2004,** *37*, 7669–7672.
23. Zois, H.; Apekis, L.; Mamunya, Y. P. Dielectric Properties and Morphology of Polymer Composites Filled with Dispersed Iron. *J. Appl. Polym. Sci.* **2003,** *88*, 3013–3020.
24. Kuzmin, D. On Evaluation of Dipole Moment of a Sphere Taking into Consideration Conductivity of Sphere

and Medium. *Izv. Vyssh. Uchebn. Zaved. Fiz.* **1968,** 136–137.
25. Halperin, W. P. Quantum Size Effects in Metal Particles. *Rev. Mod. Phys.* **1986,** *58*, 533–606.
26. Stauffer, D.; Aharony, A. *Introduction to Percolation Theory*, 2nd ed.; Taylor & Francis: London, 1994.
27. Rice, M. J.; Bernasconi, J. Gor'kov- Eliashberg Effect in One-Dimensional Metals?. *Phys. Rev. Lett.* **1972,** *29*, 113–116.
28. Carotenuto, G.; Longo, A.; Hison, C. L. Tuned Linear Optical Properties of Gold−Polymer Nanocomposites. *J. Mater. Chem.* **2009,** *19*, 5744–5750.
29. Pedersen, D. B.; Wang, S. Surface Plasmon Resonance Spectra of 2.8 Å ± 0.5 nm Diameter Copper Nanoparticles in Both Near and Far Fields. *J. Phys. Chem. C* **2007,** *111*, 17493–17499.